Detecting Moving Targets in SAR Imagery by Using a Phase-Error Correction Algorithm

J.R. Fienup and A.M. Kowalczyk

Environmental Research Institute of Michigan
P.O. Box 134001, Ann Arbor, MI 48113-4001
Internet: fienup@erim.org

ABSTRACT

Motion of a target induces phase errors in a synthetic-aperture radar (SAR) signal (phase) history that cause the image of the moving target to be smeared in azimuth. We can detect the presence of a moving target by sensing the smearing, as follows. We divide the complex image of a scene that includes a moving target into a grid of patches, and apply a phase-error correction algorithm to each patch. We have used the shear averaging phase-error correction algorithm. Patches that have large phase errors are likely to contain the image of a moving target. We also compute the sharpness of the image in the patch before and after phase-error correction; an increase in sharpness indicates the presence of a moving target, and it is a better indicator than the magnitude of the phase error. This approach requires just a single-antenna conventional SAR system. It is highly sensitive to the azimuth component of target velocity and to radial acceleration.

Keywords: synthetic aperture radar (SAR), moving-target detection, moving-target indication (MTI), phase-error correction, focusing, shear averaging

1 INTRODUCTION

Conventional methods of detecting targets moving on the ground with airborne radar systems rely on the radial component of velocity to produce Doppler shifts or on the use of displaced-phase-center antennas for background cancellation, or both.[1] In this paper we describe a new approach to detecting moving targets. It employs a single-antenna synthetic aperture radar (SAR).[2,3]. Although the approach is not sensitive to the radial component of velocity, it is highly sensitive to the along-track (azimuth) component of velocity and to radial accelerations.

2 DETECTION APPROACH

Motion of a target induces phase errors in a SAR signal (phase) history that cause the image of the moving target to smear in azimuth. We can detect the presence of a moving target by sensing the phase error or the smear. As illustrated in Figure 1, we divide the complex image of a scene into a grid of patches, and apply a phase-error correction algorithm to each patch. A patch that has a large phase error is likely to contain the image of a moving target. We also compute the sharpness of the image in the patch before and after phase-error correction; an increase in sharpness (reduction in image smearing) indicates a moving target, and this feature is superior to the magnitude of the phase error for detecting moving targets. We define the sharpness as the integrated squared intensity of the image[4] (or the fourth power of the magnitude of the complex image).

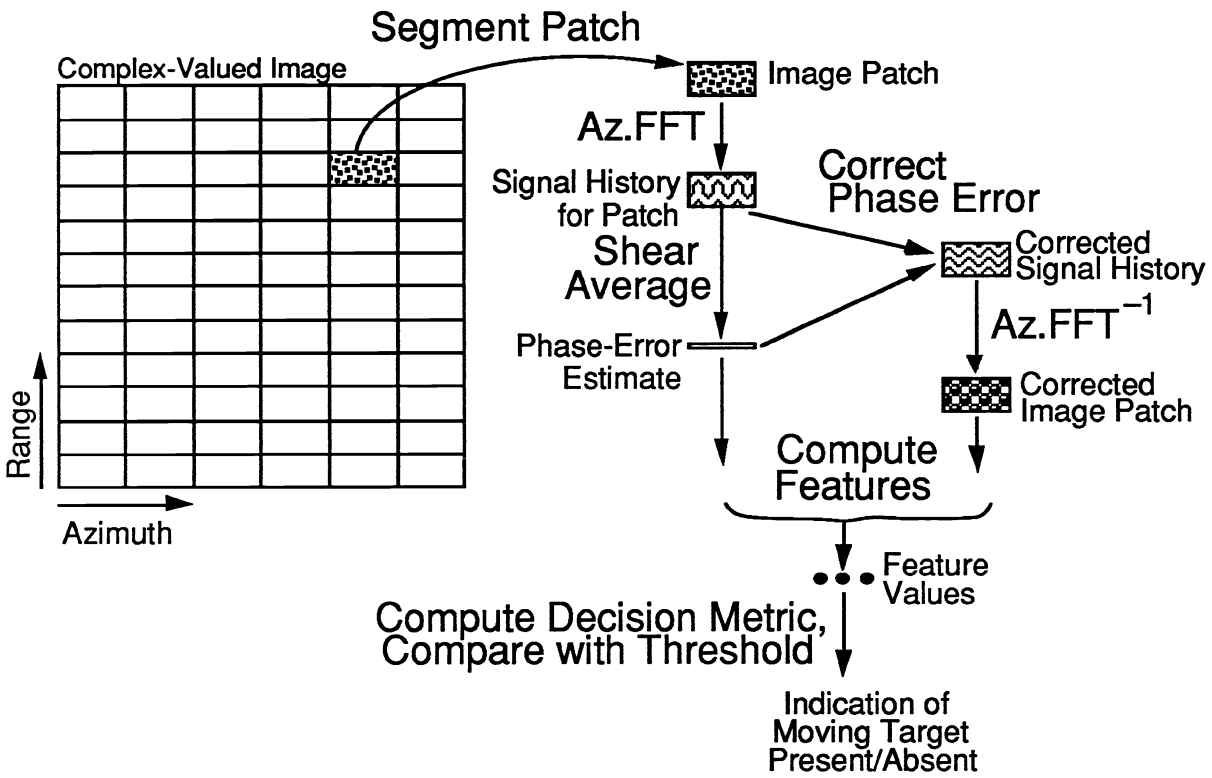

Figure 1. Flow Diagram of the Moving-Target Detection Approach

For the phase-error correction algorithm we have used the shear averaging algorithm[5] since it is computationally very fast, corrects high-order phase errors, and does not require the presence of a prominent point on the target. We can also employ other phase-error correction and focusing algorithms.[6,7]

We can also compute other features that indicate a moving target, such as the degree of image correlation, which we have found also works well but is computationally more demanding. We may also combine all the features by a likelihood ratio test to detect the moving target, if we can determine the joint statistics of the feature set.

To avoid problems with the smeared images of a moving target overlapping the boundary between two patches, we perform the detection for four overlapping grids of patches, the second offset 1/2 patch width in range from the first, the third offset by 1/2 patch length in azimuth, and the third offset in both range and azimuth.

The computational complexity of the algorithm is comparable to that of the fast Fourier transform (FFT) required to form the image, and four times that when using the four overlapping grids of patches.

3 PERFORMANCE OF THE DETECTION APPROACH

We find that the number of resolution cells the image of the target smears in azimuth is given by

$$M_a = \frac{2d_a}{\rho_a} = \frac{2v_aT}{\rho_a} \tag{1}$$

or

$$M_a = (a_rT)\frac{2T}{\lambda_o} \tag{2}$$

where

v_a = target azimuth component of velocity
T = aperture integration time
d_a = distance target travels in azimuth during aperture time
ρ_a = azimuth resolution
a_r = target radial component of acceleration
λ_o = center wavelength.

The smear caused by a radial acceleration of a_r is the same as that caused by an azimuth velocity of $v_a = (a_rT)\rho_a/\lambda_o$, and these two smears are equivalent for the purpose of detecting moving targets.

We have found that to keep a low false alarm rate we need an increased sharpness of about 2.0. Then the minimum smearing we would detect is $M_a = 2$ resolution elements, which is equivalent to a minimum azimuth velocity of $v_{amin} = \rho_a/T$ or a minimum radial acceleration of λ_o/T^2. For example, for the ADTS SAR,[8] which has resolution 0.3 m, $\lambda_o = 0.009$ m, and $T \approx 1$ sec, under ideal circumstances the minimum detectable velocity would be 0.3 m/sec (0.7 mph) and the minimum detectable radial acceleration would be 0.009 m/sec^2, which produces a change in radial velocity by 0.009 m/sec (0.02 mph) during the aperture time. From this example we see that the approach can detect targets having small azimuth components of velocity and extremely small changes in radial velocity. To detect this minimum smear the target/background ratio in the patch must be large. For smaller target/background ratios the increased sharpness ratio is given by

$$f_4 = \frac{\dfrac{K_{ta}^2\, M_aN(K_{ta} + M|\mu_g|)}{(K_{ta} + M_aM|\mu_g|)} + 2M_aM}{K_{ta}^2N + 2M_aM}, \tag{3}$$

and the minimum detectable smear is given by

$$M_{amin} = \frac{K_{ta}\beta - \sqrt{K_{ta}^2\beta^2 - 8f_{4t}(f_{4t} - 1)K_{ta}^3M^2N|\mu_g|}}{4(f_{4t} - 1)M^2|\mu_g|} \tag{4}$$

where

$$\beta = K_{ta}^2N - M(f_{4t} - 1)(2 + K_{ta}N|\mu_g|)\,. \tag{5}$$

and

K_{ta} = (total target energy)/(background energy in a single azimuth bin of the patch)
f_{4t} = sharpness increase threshold = 2.0

M = number of azimuth resolution elements in the patch
N = number of range resolution elements in the patch
$|\mu_g|$ = correlation coefficient of the background.[5]

To derive these relationships we assumed that the moving target was a delta-function reflector (such as a corner reflector) and that the presence of the focused background has caused us to underestimate the phase error due to the moving target, but the clutter background is uniform enough that its sharpness does not change much when the image patch is corrected for the phase-error estimate. The performance will be worse than this for a more highly structured background.

If a target has cross-section σ_T dbm^2, and the background has cross-section σ_o, then

$$K_{ta} = \frac{10^{\sigma_T/10}}{\rho_a \rho_r N \, 10^{\sigma_o/10}} \ , \tag{6}$$

for ρ_r and ρ_a in units of meters. For example, for a corner-reflector target with σ_T = 20 dbm^2 and a background of σ_o = –20 dB, and for N = 16 and $\rho_r = \rho_a$ = 0.3 m, we have K_{ta} = 6944 (the target image would have to be smeared over 6944 resolution elements before the target-to-background ratio in the patch would reduce to unity). If we change the resolution to $\rho_r = \rho_a$ = 3 m, and keep N = 16, then K_{ta} = 69.

As the target smearing increases with azimuth velocity or radial acceleration, the target/background ratio decreases. We have found that the maximum detectable smear is limited by the need to have the total target energy be at least half the total background energy in the patch, for the case of a uniform clutter background. That target/background ratio would have to exceed four for the most highly structured background. Performance degrades further if some of the target energy smears outside the patch. In that situation we can increase the maximum detectable velocity or acceleration by processing the data to a coarser resolution (using a shorter aperture time), thereby causing the length of the smear to decrease. Coarser resolutions increase the minimum detectable velocity as well; consequently we desire the finest resolution SAR image when detecting slowly moving targets.

4 DETECTION EXAMPLE

We applied our detection algorithm, employing the increased sharpness feature, to an image collected by MIT Lincoln Laboratory's ADTS 33.56 GHz SAR, which has one-foot resolution in both range and azimuth.[8,9] The image contained a schoolbus moving in a circular path. The image was 2048 pixels in range by 708 pixels in azimuth. We processed the range-compressed data into an image by simply Fourier transforming in azimuth. Since polar interpolation is necessary to produce a full-resolution image, the images we produced have degraded resolution away from the center of the scene. Nevertheless, the image is adequate for demonstrating our detection algorithm. Figure 2 shows the magnitude of the ADTS image. Figure 3 shows the detection result, for which we used a patch size of 32 pixels in range by 128 pixels in azimuth. The small rectangles seen in Figure 3 are 1/2 this size in each dimension because of the effect of averaging the four overlapping patches. We ordinarily display the increased sharpness ratio as a false-color image with the color indicating the value of

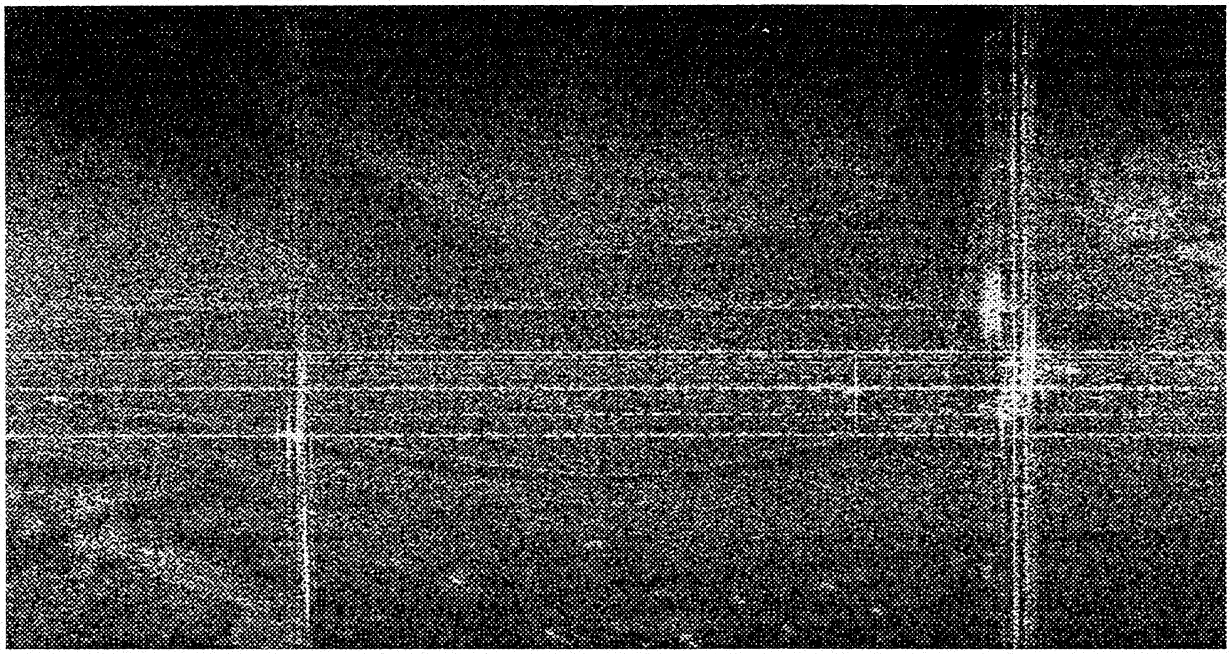

Figure 2. ADTS Image. Range increases from left to right. The vertically smeared image of a moving schoolbus is located along the lower edge of the image on the left.

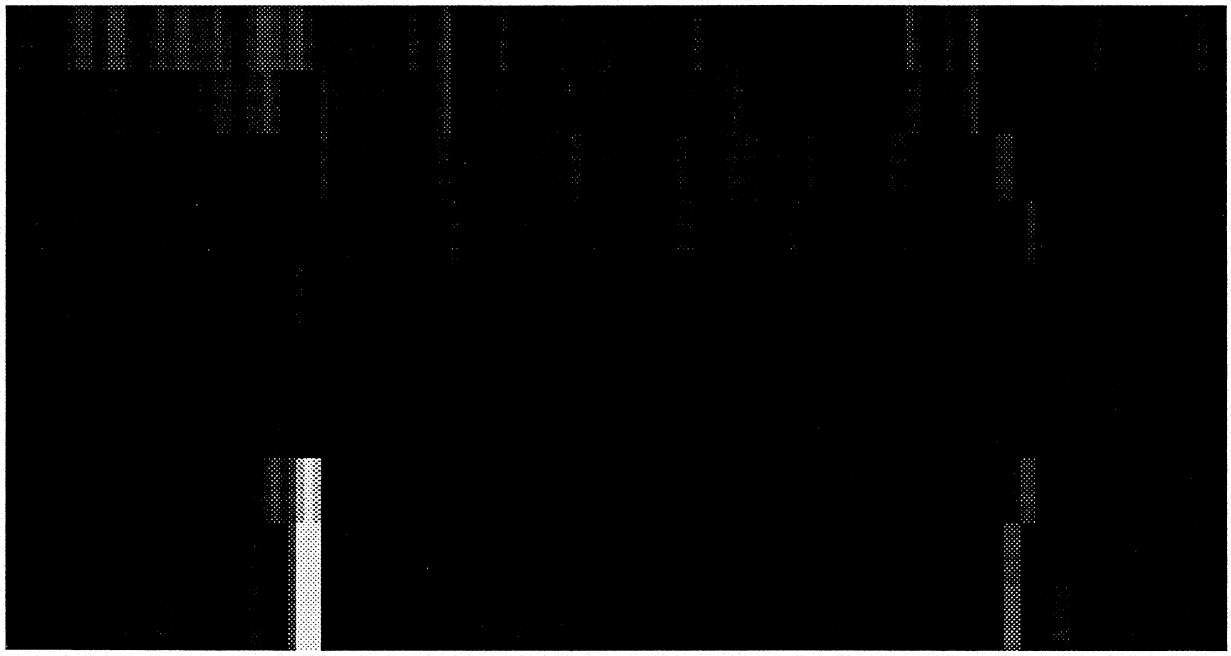

Figure 3. Results of Moving-Target Detection Algorithm. White rectangles indicate patches likely to contain images of moving targets. Only the area including the smeared image of the schoolbus is indicated as containing a moving target.

increased sharpness ratio and with the brightness proportional to the image magnitude. However, to avoid the difficulty in reproducing color photographs, we here show a separate array that indicates the increased sharpness of the patch as a gray level, with white indicating sharpness increase of two or above (moving target present with high probability), black indicating sharpness increase of unity or below (moving target absent), and gray levels indicating intermediate values. Since we used four overlapping grids of patches, we show the average value of the sharpness increase from the four patches in which each pixel falls.

Only in the area in which the smeared image of the schoolbus appears does the algorithm indicate the presence of a moving target (white area in Figure 3). Other bright non-moving targets in the image are not indicated as moving targets — there are no false alarms in this case. Figure 4 shows the same thing in a perspective plot. The maximum value of increased sharpness is 6.2, more than three times the typical threshold of 2.0, giving a strong indication of a moving target.

In some other cases we have missed targets; for example, if the smearing is highly spatially variant (different for different parts of the target) then a simple phase-error-correction algorithm cannot focus all of it at once, and the sharpness may not increase sufficiently. We have also encountered some false alarms. For example, a guard rail along a gently curving road may create a glint off the part that is perpendicular to the instantaneous line of site, and this glint moves as the SAR platform advances, causing a false indication of a moving target.

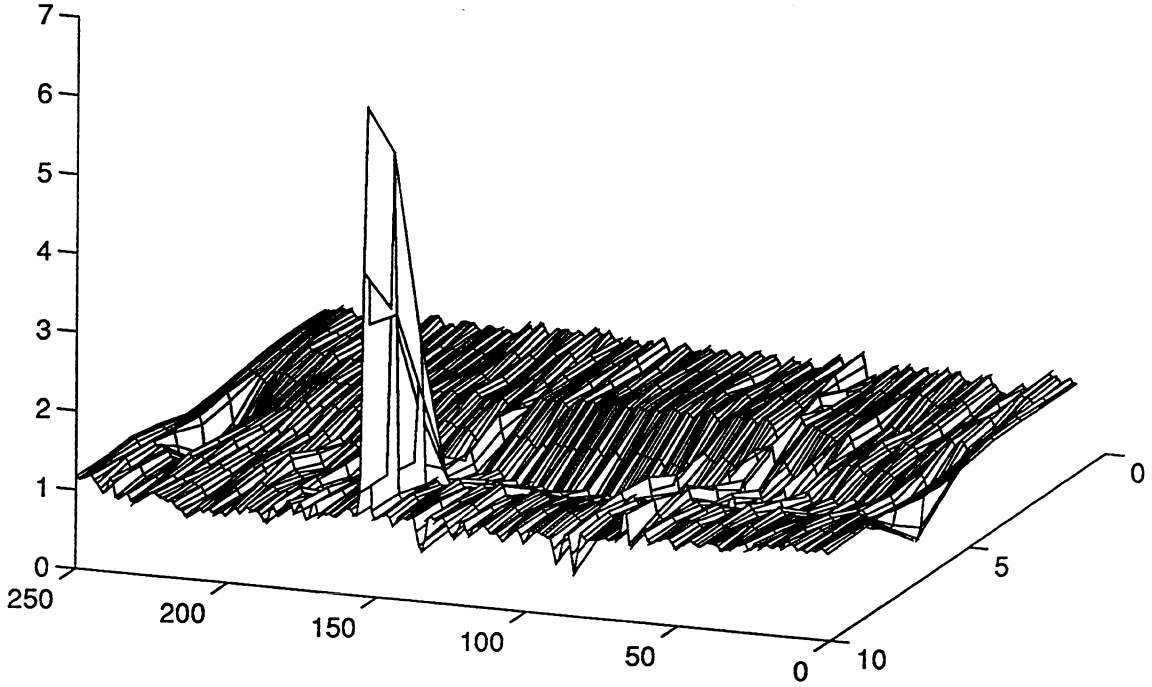

Figure 4. Detection Result. Areas having increased sharpness of about 2.0 or greater are likely to contain moving targets.

5 CONCLUSIONS

We have developed a new approach for detecting moving targets that depends on the ability to focus smeared images of moving targets from a single-antenna SAR system. It is highly sensitive to

azimuth components of velocity and to radial components of acceleration. We have successfully demonstrated the approach on an image of a moving schoolbus taken with the ADTS SAR.

ACKNOWLEDGMENTS

C. Bobrowski and N.L. Kay assisted in the coding of the moving-target detection software. We thank John Henry, MIT Lincoln Laboratory, for providing ADTS data on the moving schoolbus. This effort was supported by ERIM Internal Research and Development funds.

REFERENCES

1. M.I. Skolnik, Radar Handbook, Second Edition (McGraw-Hill, 1990).

2. J.L. Walker, "Range-Doppler Imaging of Rotating Objects," IEEE Trans. Aerosp. and Electr. Sys. AES-16, 23-52 (1980).

3. D.A. Ausherman, A. Kozma, J.L. Walker, H.M. Jones and E.C. Poggio, "Developments in Radar Imaging," IEEE Trans. AES-20, 363-400 (1984).

4. R.A. Muller and A. Buffington, "Real-Time Correction of atmospherically Degraded Telescope Images through Image Sharpening," J. Opt. Soc. Am. 64, 1200-1210 (1974).

5. J.R. Fienup, "Phase Error Correction by Shear Averaging," in Signal Recovery and Synthesis III, digest of papers (Optical Society of America, 1989), pp. 134-137.

6. S.A. Werness, W.G. Carrara, L. Joyce and D. Franczak, "Moving Target Imaging Algorithm for SAR Data," IEEE Trans. AES 26, 57-67 (1990).

7. P.H. Eichel, D.C. Ghiglia and C.V. Jakowatz, Jr., "Speckle Processing Method for Synthetic-Aperture-Radar Phase Correction," Opt. Lett. 14, 1-3 (1989).

8. John C. Henry, "The Lincoln Laboratory 35 GHz Airborne Polarimetric SAR Imaging Radar System," IEEE Aerospace & Electronics Systems Society, 1991 National Telesystems, Atlanta, GA., 26 March 1991.

9. D.P. Morrison, A.C. Eckert, and F.J. Shields, "Studies of Advanced Detection Technology Sensor (ADTS) Data," in Algorithms for Synthetic Aperture Radar Imagery, D.A. Giglio, ed., Proc. SPIE 2230, 370-378 (1994).